transport to the substrate; (iii) particle–particle and particle–substrate sintering.

In considering some of the basic mechanisms involved it should be noted that the generated aerosol faces competing processes of evaporation, coagulation and particle settling. The addition of turbulent fluid flow, chaotic aerosol generation, and laser interaction with reactant chemicals makes the prediction of particle deposition intractable. However, the evaporation lifetime of an aerosol particle can be expressed by

$$t = \frac{R\rho d^2}{8DM(P_p/T_p - P/T)}$$

where R is the gas constant, ρ is the particle density, d is the particle diameter, D is the vapor diffusion coefficient, M is the molecular weight, P_p is the partial pressure at the drop, P is pressure at infinite distance, T_p is the temperature at the drop, and T is temperature at infinite distance. Therefore, the lifetime is proportional to the square of the diameter. For particles of similar size the coagulation will obey the Brownian equation

$$N(t) = \frac{N_0}{1 + N_0kt}$$

where $N(t)$ is the number of particles at time t, N_0 is the initial number of particles, and k is the coagulation coefficient. Through this process the number of particles will decrease as the reciprocal of time. The deposition rate from the aerosol on a surface is given by

$$n(t) = 2n_0(Dt/\pi)^{1/2}$$

where $n(t)$ is the number of particles per unit surface area at time t, n_0 is the initial number available, and D is the diffusion coefficient given by

$$D = \frac{\kappa TC}{3\pi\eta d}$$

where T is temperature, C is the slip correction factor, d is the diameter, η is the viscosity, and κ is Boltzmann's constant. The slip correction factor is given by

$$C = 1 + \lambda/d(2.514 + 0.8\exp(-0.55d/\lambda))$$

where λ is the mean free path of the gas. This leads to the conclusion that the deposition rate depends upon the square root of time and the temperature/viscosity ratio. Future work will investigate the validity of this prediction.

Conclusion

It has been demonstrated that laser synthesis can be used to form amorphous silicon nitride coatings on nickel, titanium, copper, and silica substrates. The method involves the pyrolysis of a molecular precursor to form aerosol droplets that condense into 85–500-mm silicon nitride particles. Following arrival at the substrate, these particles undergo laser-induced sintering, thereby producing a strong, highly adherent surface coating.

Acknowledgment. This work was supported in part by the donors of the Petroleum Research Fund, administered by the American Chemical Society, at Stevens Institute and the Office of Naval Research under Contract N00014-C-0580 at the University of Connecticut. We thank Dr. S. Patel for determining the extinction coefficient of the silazane monomer.

Registry No. Ni, 7440-02-0; Ti, 7440-32-6; Cu, 7440-50-8; SiO_2, 7631-86-9; silicon nitride, 12033-89-5.

Synthesis of Thin Films by Atmospheric Pressure Chemical Vapor Deposition Using Amido and Imido Titanium(IV) Compounds as Precursors

Renaud M. Fix, Roy G. Gordon,* and David M. Hoffman*

Department of Chemistry, Harvard University, 12 Oxford Street, Cambridge, Massachusetts 02138

Received November 2, 1989

In an attempt to prepare TiN, the amido- and imidotitanium(IV) complexes $Ti(NR_2)_4$ (R = Me or Et), $Ti(NMe_2)_3(t\text{-Bu})$, and $[Ti(\mu\text{-N-}t\text{-Bu})(NMe_2)_2]_2$ were used as precursors in an atmospheric pressure chemical vapor deposition process. Depositions on glass, silicon, vitreous carbon, and boron substrates were successfully carried out at temperatures below 450 °C to give coatings up to 6000 Å thick and growth rates from 50 to 1000 Å/min. The films, which were characterized by electron microprobe and Rutherford backscattering, contained titanium and nitrogen in a ratio close to 1, plus significant amounts of carbon and oxygen. X-ray photoelectron analyses with depth profiling confirmed that the films are uniform in composition, the nitrogen is Ti bound, and the carbon is both Ti bound and organic. The analyses indicate precursor decomposition mechanisms involving both Ti–NR_2 homolytic bond cleavage and amido ligand β-hydride activation, the latter accounting for the presence of Ti-bound carbon in the films. In support of this hypothesis, films made from precursors with cyclic amido ligands, for which β-hydride activation is disfavored, contained only organic carbon.

Introduction

Titanium nitride, TiN, displays an interesting combination of properties.[1] For instance, the optical properties of TiN resemble those of gold, yet it is harder than all elemental metals and sapphire (Al_2O_3) and almost as hard as diamond. Its melting point is almost 3000 °C, which is higher than that of most materials, and it is inert to most chemicals and solvents except aqua regia, which dissolves it slowly, and HF. Titanium nitride is a better electrical conductor than titanium metal.

(1) Refractory Materials; Margrave, J. L., Ed.; Academic Press: New York, 1971.

0897-4756/90/2802-0235$02.50/0

Because of their unique properties, TiN thin films have been utilized for several technological applications. For example, they are widely used as wear-resistant coatings on machine tools and as decorative (gold-colored) coatings on watches and jewelry. Possible applications of TiN films include their use as diffusion barriers or as electrical connections in microelectronics and solar cells. Titanium nitride is also a candidate for use as a solar control coating on windows in warm climates.

Atmospheric pressure chemical vapor deposition (APCVD) is a widely used method for synthesizing coatings because it is a simple and inexpensive technique that generally gives high growth rates, good step coverage, and powder-free films. There are several APCVD routes to TiN films available,[2] but only the method of Gordon and Kurtz gives high quality TiN coatings at high growth rates and temperatures as low as 500 °C (eq 1).[3] The low

$$6TiCl_4 + 8NH_3 \xrightarrow{500\text{–}700\ °C} 6TiN + 24HCl + N_2 \quad (1)$$

temperature range required for reaction 1 is important because it permits depositions to be carried out on thermally sensitive substrates such as silicon chips, solar cells, and glass.

If TiN thin films are to be applied on more thermally sensitive substrates such as aluminum-metallized chips, amorphous silicon solar cells, and plastics, then reactions that require still lower deposition temperatures are needed. With these sorts of applications in mind, we decided to examine the possibility that nitrogen-containing inorganic and organometallic precursors might permit the low-temperature (<400 °C) deposition of TiN.

One class of possible precursors are the volatile tetrakis(dialkylamido)titanium(IV) complexes, $Ti(NR_2)_4$. Two of these compounds, $Ti(NMe_2)_4$ and $Ti(NEt_2)_4$, have in fact been used by Sugiyama et al. to deposit films at temperatures as low as 300 °C.[4,5] Their films contain titanium and nitrogen but also carbon and oxygen contamination. In general, the presence of carbon and oxygen degrades the properties of TiN films; for instance, it increases electrical resistance and decreases hardness.

The purpose of the present study was 2-fold. First, we wanted to develop some understanding of the problems associated with the use of $Ti(NR_2)_4$ (R = Me and Et) precursors, especially with regard to carbon contamination.[4] For instance, by determining the nature of the carbon in the coatings made from these compounds (i.e., is it in the form of carbide, organometallic carbon, or organic carbon?), we could infer a mechanism of precursor decomposition and use this as a basis for the modification of existing precursors and the design of new ones. Second, we wanted to experimentally test our mechanistic hypotheses by preparing films using the newly designed precursors.

In our work we have been partially successful; we appear to have circumvented one of two primary pathways that result in carbon contamination of films made from $Ti(NMe_2)_4$ and $Ti(NEt_2)_4$, but the other still leaves carbon in the films. Adjunct to our primary objectives, we also show that with the use of boron substrates, Rutherford backscattering is an excellent technique for the quantitative analysis of carbon, nitrogen, and oxygen in thin films.

Experimental Section

Synthesis. All syntheses were performed under a prepurified nitrogen atmosphere using standard Schlenk techniques or an inert-atomosphere glovebox. Solvents used in the preparations were purified by standard techniques and were dry and oxygen free. NMR spectra were recorded on Brucker instruments (AM-300 and AM-500). ^1H NMR chemical shifts are reported relative to the ^1H impurity in the solvent (benzene-d_6, δ 7.15). Infrared spectra are referenced externally to the 1601-cm^{-1} band of polystyrene. Microanalyses were performed by Oneida Research Services Inc., Whitesboro, NY.

The compounds $Ti(NMe_2)_4$ (**1**), $Ti(NEt_2)_4$ (**2**), $[Ti(N\text{-}t\text{-}Bu)(NMe_2)_2]_2$ (**6**), and $Ti(NC_5H_{10})_4$ (**5**, tetrakis(piperidino)titanium) were synthesized as described by Bradley and co-workers.[6] Tetrakis(pyrrolidino)titanium (**4**, $Ti(NC_4H_8)_4$), which has not been previously reported, was synthesized as follows. $TiCl_4$ (2.94 g, 15.5 mmol) in toluene (15 mL) was added to a slurry of $LiNC_4H_8$ (6.74 g, 87.5 mmol) in ether (50 mL) at 0 °C. The mixture was allowed to warm to room temperature slowly and then refluxed for 2 h. The solvents were then removed in vacuo, and the residue was extracted with pentane (3 × 50 mL) and filtered (Celite). The filtrates were combined, and the pentane was then removed in vacuo, leaving a dark green oily liquid (4.9 g, 96%) which was >95% pure $Ti(NC_4H_8)_4$ by ^1H NMR spectroscopy. The material used for CVD and the chemical analysis was purified by vacuum distillation (yellow–orange oily liquid; bp 160 °C/0.05 mmHg; yield 50%). Anal. Calcd for $TiN_4C_{16}H_{32}$: N, 17.06; C, 58.53; H, 9.82. Found: N, 16.92; C, 58.74; H, 9.68. ^1H NMR (C_6D_6) δ 1.55 (m, 4, NCH_2CH_2), 3.78 (m, 4, NCH_2CH_2); IR (neat, KBr, cm^{-1}) 2680 b, 2595 w, 1500 s, 1320 s, 1280 m, 1235 b, 1180 b, 1070 s, 1025 s, 950 b, 715 m.

$Ti(NMe_2)_3(t\text{-}Bu)$ was prepared by the addition of Li-*t*-Bu in hexane (7.14 mmol) to $Ti(NMe_2)_4$ in hexane (1.39 g, 6.18 mmol) at 0 °C.[7,8] After the addition was complete, the mixture was allowed to warm to room temperature. It was filtered through a glass frit, and the solvent then removed in vacuo leaving a dark orange oil. The compound was purified by vacuum distillation (orange oil; bp 80 °C/0.1 mmHg; yield 60%). Anal. Calcd for $TiN_3C_{10}H_{27}$: N, 17.71; C, 50.63; H, 11.47. Found: N, 17.12; C, 50.02; H, 11.30. ^1H NMR (C_6D_6) δ 1.23 (s, 9, $C(CH_3)_3$), 3.09 (s, 18, $N(CH_3)_2$); IR (neat, KBr, cm^{-1}) 2930 b, 2870 b, 2830 b, 2780 s, 2700 w, 1445 b, 1420 m, 1350 w, 1250 s, 1145 s, 1120 m, 1055 m, 940 s, 790 m, 590 s.

Tetrakis(diallylamido)titanium(IV), $Ti[N(CH_2CHCH_2)_2]_4$, which has not been previously reported, was synthesized as follows. $TiCl_4$ (2.94 g, 15.5 mmol) in toluene (15 mL) was added to a slurry of $LiN(CH_2CHCH_2)_2$ (9.12 g, 87.5 mmol) in ether (50 mL) at 0 °C. The mixture was allowed to warm to room temperature slowly and then refluxed for 2 h. The solvents were then removed in vacuo, and the residue was extracted with pentane (3 × 50 mL) and filtered (Celite). The filtrates were combined, and the pentane was then removed in vacuo, leaving a dark red oily liquid that was >90% pure $Ti[N(CH_2CHCH_2)_2]_4$ by ^1H NMR spectroscopy (yield 70%). The compound decomposed upon heating, leaving an insoluble red solid (polymerization?), thus preventing further purification by distillation. Anal. Calcd for $TiN_4C_{24}H_{40}$: N, 12.95; C, 66.65; H, 9.32. Found: N, 12.76; C, 67.02; H, 9.64. ^1H NMR (C_6D_6) δ 4.15 (d, 4, J_{HH} = 7.56 Hz, $N(CH_2CHCH_2)_2$), 5.08 (m, 4, $N(CH_2CHCH_2)_2$), 5.80 (m, 2, $N(CH_2CHCH_2)_2$); IR (neat, KBr, cm^{-1}) 3030 s, 2800 vs, 2605 m, 2525 w, 2390 vw, 2300 vw, 1835 m, 1620 s, 1575 vs, 1550 s, 1530 m, 1515 w, 1470 w, 1450 m, 1415 s, 1400 s, 1310 m, 1265 w, 1185 w, 1115 w, 1070 w, 1050 w, 975 w, 900 m, 685 m.

CVD Apparatus and Procedure. The depositions were carried out in an atmospheric-pressure laminar-flow rectangular

(2) (a) Schintlmeister, W.; Pacher, O.; Pfaffinger, K. *J. Electrochem. Soc.* **1976**, *123*, 924. (b) Bernex A. G. Olten, Switzerland, Data sheet on Moderate-Temperature CVD of Ti(C,N) Coatings.

(3) Kurtz, S. R.; Gordon, R. G. *Thin Solid Films* **1983**, *140*, 277.

(4) Sugiyama, K.; Pac, S.; Takahashi, Y.; Motojima, S. *J. Electrochem. Soc.* **1975**, *122*, 1545.

(5) The preparation of thin films from titanium complexes with other types of nitrogen-bearing ligands: Morancho, R.; Constant, G.; Ehrhardt, J. J. *Thin Solid Films* **1981**, *77*, 155. Morancho, R.; Constant, G. *C. R. Acad. Sci., Ser. C* **1977**, *285*, 77. Morancho, R.; Petit, J. A.; Dabosi, F.; Constant, G. *J. Electrochem. Soc.* **1982**, *129*, 854.

(6) (a) Bradley, D. C.; Thomas, I. M. *J. Chem. Soc.* **1960**, 3857. (b) Bradley, D. C.; Torrible, E. G. *Can. J. Chem.* **1963**, *41*, 134.

(7) Manzer, L. E. Patent 4,042,610, 1977.

(8) Related $Ti(NR_2)_3R'$ compounds: Bürger, H.; Neese, H.-J. *J. Organomet. Chem.* **1969**, *20*, 129.

Table I. Typical CVD Conditions and Growth Rates

precursor	temp of precursor, °C	carrier gas	linear flow, m/min	dep temp, °C	growth rate, Å/min
$Ti(NMe_2)_4$	20	N_2	1.4	400	195
$Ti(NMe_2)_4$	55	N_2	1.0	400	630
$Ti(NMe_2)_4$	70	He	5.0	400	1000
$Ti(NMe_2)_3(t\text{-Bu})$	60	N_2	1.4	400	250
$Ti(NMe_2)_3(t\text{-Bu})$	60	N_2	1.4	350	220
$Ti(NEt_2)_4$	70	He	5.0	400	400
$[Ti(\mu\text{-N-}t\text{-Bu})(NMe_2)_2]_2$	120	He	5.0	400	~50

Table II. Precursor Volatility Data

precursor	boiling point, °C/pressure, mmHg
$Ti(NMe_2)_4$	60/0.1
$Ti(NEt_2)_4$	100/0.1
$Ti(NMe_2)_3(t\text{-Bu})$	80/0.1
$Ti(NC_4H_8)_4$	160/0.05
$Ti(NC_5H_{10})_4$	mp 70; bp 180/0.05[a]
$[Ti(\mu\text{-N-}t\text{-Bu})(NMe_2)_2]_2$	sublimes 140/0.1

[a] Reference 6.

reactor that has been previously described.[3] The precursors were loaded in a glass bubbler except for the precursor $[Ti(\mu\text{-N-}t\text{-Bu})(NMe_2)_2]_2$, which was injected as a hexane solution into a hot zone (150 °C) located just before the CVD chamber. Ultrahigh-purity helium or nitrogen passed through a Nanochem gas purifier (Model L-50 t) was used as carrier gas. The system, loaded with the substrates, was purged for at least 2 h before each deposition. Under these conditions, analyses of the helium outflow showed that it contained less than 0.5 ppm O_2 and H_2O. After each deposition the films were allowed to cool slowly in the reactor under a flow of helium. Preheating of the precursors or carrier gas was accomplished by wrapping the bubbler and tubing with heating tape.

Silicon substrates were cleaned by immersion in H_2O_2:H_2SO_4 (1:4) for 10 min and then dilute HF until hydrophobic. Deionized water was used for final rinsings. The vitreous carbon and boron substrates, which were obtained from Atomergic Chemetals Corp., were degreased in $C_2F_3Cl_3$. The glass substrates were Corning 7059 low-sodium glass. They were etched for 1 min in HF/HNO_3 (1:10) and then rinsed with deionized water.

Film Characterization. A sheet resistance meter (Veeco four-point probe) was used for resistivity measurements. X-ray diffraction was performed on a Guinier thin-film goniometer (Model 651). Electron microprobe analyses (EMA) were performed on a Cameca MBX system. Rutherford backscattering (RBS) analyses (General Ionics Model 4117) were performed using a beam of He^+ of energy 2.0 MeV for films deposited on silicon and vitreous carbon and 1.8 MeV for films deposited on boron. X-ray photoelectron spectroscopy (XPS) was carried out using a Surface Science Lab SSX-100 system equipped with a 3-keV Ar^+ sputter gun. The electron-energy analyzer was calibrated to the Au $4f_{7/2}$ line at 84 eV. XP spectra were collected in the unscanned mode by using the monochromatized Al Kα excitation with a spot size 600 μm and the electron-energy analyzer set for a pass energy of 150 eV. The experimental detector width is 18.6 eV in this configuration. The base pressure was 10^{-7} Torr with the Ar^+ gun on.

Chart I

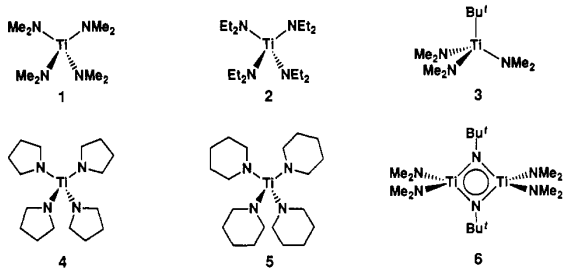

Results and Discussion

Films were prepared by using compounds **1**–**6** as precursors (Chart I). Precursors **1**, **2**, **5**, and **6** were prepared as described in the literature.[6] Precursor **4** is a new compound and was prepared by a method analogous to the one used to synthesize **1** and **2**.[6] Compound **3** is also new. It was synthesized according to eq 2 and purified by vacuum distillation (bp 80 °C/0.1 mmHg).[7]

$$Ti(NMe_2)_4 + \text{Li-}t\text{-Bu} \xrightarrow{\text{hexane}} Ti(NMe_2)_3(t\text{-Bu}) + LiNMe_2 \quad (2)$$

In general, depositions were successfully carried out at temperatures from 350 to 450 °C on glass, silicon wafer, vitreous carbon, and boron substrates (Table I). Using $Ti(NMe_2)_3(t\text{-Bu})$ as the precursor, a smooth, adherent film was deposited at 300 °C. Presumably the lower deposition temperature for this compound reflects the availability of facile pathways for loss of the *t*-Bu ligand (e.g., alkyl β-hydrogen elimination or Ti–CMe_3 homolytic cleavage). Attempts to deposit films at temperatures below 350 °C using $Ti(NMe_2)_4$ or $Ti(NEt_2)_4$, as previously reported by Sugiyama,[4] gave powdery coatings that did not adhere to the substrates. Growth rates, which ranged from 50 to 1000 Å/min, were dependent on the volatility of the precursors (Table II). The growth rates could be increased by preheating the carrier gas and precursor, but with extensive heating, powder formation increased without an increase in film growth rate.

In general, the films were smooth and nonporous and showed good adhesion (Scotch tape test). They were optically absorbent and conductive, but were 5–10 times more electrically resistant than pure CVD TiN films prepared at higher temperatures (TiN, 300 $\mu\Omega$ cm, as reported by Gordon and Kurtz).[3] X-ray diffraction studies showed that the films were amorphous, which may be due to the low temperature of deposition. The films were chemically stable; they were etched slowly by aqua regia and could be dissolved only under vigorous conditions (HF/HNO_3 solution).

Analyses of the films were carried out using Rutherford backscattering spectrometry (RBS), X-ray photoelectron

Table III. Electron Microprobe Analysis Data for Films Obtained from $Ti(NMe_2)_4$, $Ti(NMe_2)_3(t\text{-Bu})$, and $[Ti(\mu\text{-N-}t\text{-Bu})(NMe_2)_2]_2$

precursor	t,[a] °C	Ti,[b] at. %	N, at. %	C, at. %	O, at. %	N/Ti	C/Ti	O/Ti
$Ti(NMe_2)_4$	500	26	25	35	14	1.0	1.4	0.6
$Ti(NMe_2)_4$	450	25	27	35	13	1.1	1.4	0.5
$Ti(NMe_2)_4$	420	23	27	33	17	1.2	1.5	0.8
$Ti(NMe_2)_4$	400	22	29	32	17	1.3	1.5	0.8
$Ti(NMe_2)_4$	350	22	28	32	18	1.3	1.5	0.9
$Ti(NMe_2)_3(t\text{-Bu})$	400	24	27	36	13	1.1	1.5	0.5
$Ti(NMe_2)_3(t\text{-Bu})$	350	22	26	33	18	1.2	1.5	0.8
$Ti(NMe_2)_3(t\text{-Bu})$	300	20	22	29	29	1.2	1.5	1.5
$[Ti(\mu\text{-N-}t\text{-Bu})(NMe_2)_2]_2$	450	24	28	30	18	1.1	1.2	0.8
$[Ti(\mu\text{-N-}t\text{-Bu})(NMe_2)_2]_2$	400	24	25	34	16	1.0	1.4	0.7

[a] Substrate temperature; all depositions on low-sodium glass. [b] Atom percent composition.

Table IV. RBS Data for Films Obtained from $Ti(NMe_2)_4$, $Ti(NEt_2)_4$, and $Ti(NC_4H_8)_4$

precursor	substrate	t[a] °C	Ti,[b] at. %	N, at. %	C, at. %	O, at. %	N/Ti	C/Ti	O/Ti	C/N
$Ti(NMe_2)_4$	B	400	21	25	34	20	1.2	1.7	0.9	1.4
$Ti(NEt_2)_4$	C	400	22	19	33	26	0.9	1.5	1.2	1.7
$Ti(NEt_2)_4$	B	400	17	19	41	23	1.1	2.5	1.4	2.2
$Ti(NC_4H_8)_4$	B	400	15	18	50	16	1.2	3.3	1.1	2.7

[a] Substrate temperature. [b] Atom percent composition.

Table V. XPS Analysis Data

precursor	substrate	t,[a] °C	Ti,[b] at. %	N, at. %	C, at. %	O, at. %	N/Ti	C/Ti	O/Ti	C/N
$Ti(NMe_2)_4$	B	400	29	19	23	29	0.7	0.8	1.0	1.2
$Ti(NMe_2)_4$	Si	400	25	21	42	12	0.8	1.6	0.5	2.0
$Ti(NMe_2)_4$	glass	420	28	19	34	20	0.7	1.2	0.7	1.8
$Ti(NMe_2)_3(t\text{-Bu})$	Si	400	26	24	30	20	0.9	1.1	0.8	1.2
$Ti(NMe_2)_3(t\text{-Bu})$	Si	350	25	24	32	19	0.9	1.3	0.8	1.3
$Ti(NMe_2)_3(t\text{-Bu})$	Si	300	23	19	32	26	0.8	1.4	1.1	1.7
$[Ti(N\text{-}t\text{-Bu})(NMe_2)_2]_2$	Si	450	25	22	35	18	0.9	1.4	0.7	1.6
$Ti(NEt_2)_4$	Si	400	23	15	41	21	0.7	1.8	0.9	2.7
$Ti(NEt_2)_4$	B	400	26	15	28	31	0.6	1.1	1.2	1.9
$Ti(NC_5H_{10})_4$	glass	650	15	9	66	10	0.6	4.3	0.7	7.1
$Ti(NC_5H_{10})_4$	Si	400	14	9	56	21	0.7	4.0	1.5	6.0
$Ti(NC_4H_8)_4$	glass	400	20	13	39	28	0.6	1.9	1.4	3.0

[a] Substrate temperature. [b] Atom percent composition.

spectroscopy (XPS), and electron microprobe analysis (EMA). Table III is a summary of the EMA results for **1**, **3**, and **6**; EMA data could not be obtained for **2**, **4**, and **5** because the films were not conductive enough or too thin (<3000 Å). According to the EMA results, the Ti/N ratio for **1**, **3**, and **6** is close to 1, but there is significant carbon and oxygen contamination. Interestingly, the EMA data show that the films synthesized from $Ti(NMe_2)_3(t\text{-Bu})$ and $Ti(NMe_2)_4$ had similar amounts of carbon contamination; that is, the presence of the extra carbon in the precursor $[Ti(NMe_2)_3(t\text{-Bu})$ vs $Ti(NMe_2)_4]$ did not result in significantly more carbon contamination of the films.

In the EMA technique, the nitrogen line is obscured by titanium, and the nitrogen concentration must be evaluated by difference. RBS data were therefore obtained to have analytical data complementary to the EMA results and to provide primary analytical data for films made from **2** and **4**. RBS also provided film thickness and nondestructive depth profile information.

Film thicknesses, which were in the range 1000–5000 Å, and depth profile data for titanium were readily obtained from the RBS spectra for films deposited on silicon wafer substrates, but the actual chemical composition of the films could not be reliably calculated due to the large Si background (e.g., Figure 1) that obscured the light element peaks (C, N, O). As illustrated by the examples in Figure 2, this difficulty was circumvented by examining films deposited on vitreous carbon (Figure 2a) and boron (Figure 2b). It should be noted that boron gives a low-energy nuclear reaction with He^+ at a nuclear resonance of 2.06 MeV.[9] For this reason, RBS spectra were obtained for the boron substrates by using a He^+ beam energy of 1.8 MeV.

The chemical compositions calculated from RBS spectra for films made from $Ti(NEt_2)_4$ revealed that the amount of carbon incorporation is greater for $Ti(NEt_2)_4$ than for $Ti(NMe_2)_4$. For the other films, the RBS chemical composition data (Table IV) confirmed the EMA results presented in Table III. The RBS spectra also showed that that all elements are distributed uniformly in the film (e.g., see Figure 2b). In particular, carbon and oxygen are not simply on the surface, suggesting they are incorporated during deposition as opposed to postdeposition. Oxygen

(9) Lee, Jr., L. L.; Schiffer, J. P. *Phys. Rev.* **1959**, *115*, 160.

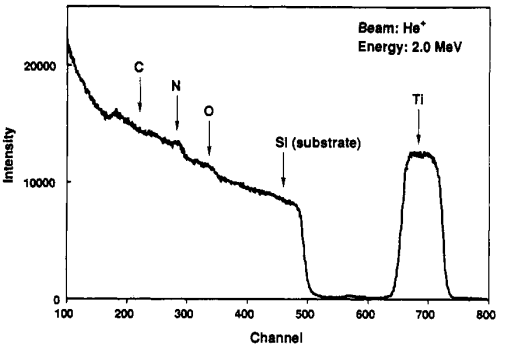

Figure 1. Example of a RBS spectrum for a film containing Ti, N, C, and O deposited on a silicon wafer.

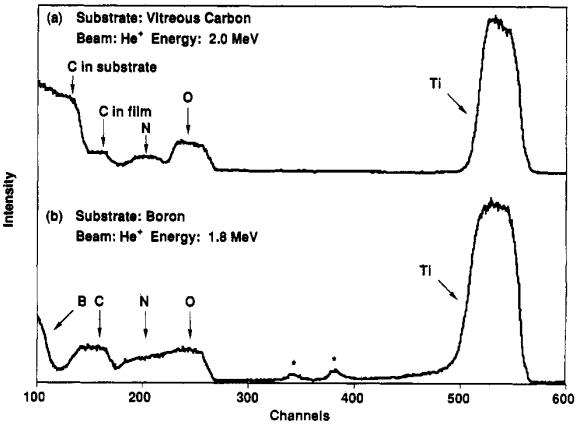

Figure 2. RBS spectra for films of approximately the same thickness deposited at 400 °C on vitreous carbon (a) and on boron (b) with **2** as precursor. The starred peaks in b are present in spectra obtained for clean boron substrates.

incorporation probably results from traces of O_2 and/or H_2O in the carrier gas or absorbed in the walls of the reactor, whereas carbon undoubtedly comes from the molecular precursors.

XPS depth profile data for the films were obtained to determine the light-element chemical bonding and to confirm chemical compositions. Chemical compositions

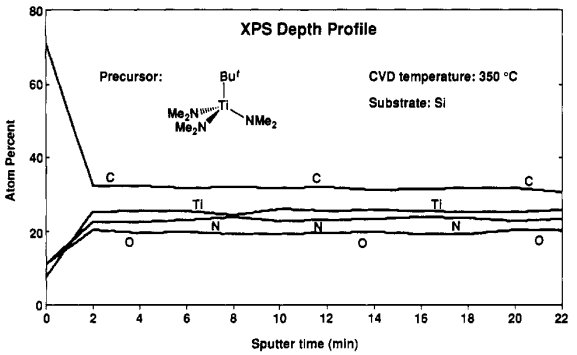

Figure 3. XPS depth profile for a film deposited at 350 °C on a silicon wafer with **3** as precursor.

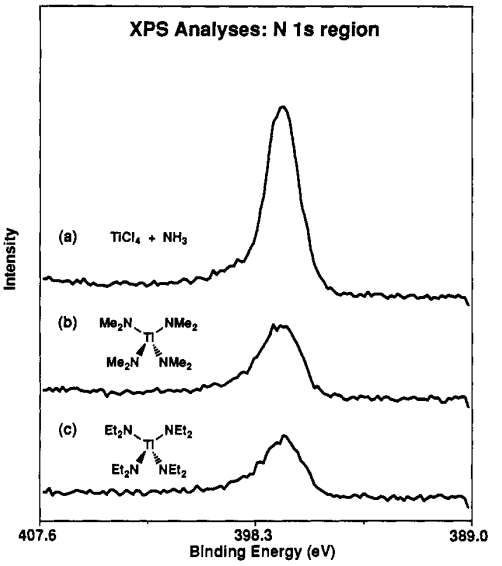

Figure 4. N 1s region of the XPS spectra for pure TiN (a) and for films deposited on silicon wafers at 400 °C with **1** (b) and **2** (c) as precursors.

as calculated from the XPS spectra (after a fixed sputter time) are given for some representative films in Table V. The compositions did not vary appreciably with sputter time (e.g., see Figure 3), which is consistent with the RBS results. The data presented in Table V, therefore, are representative of the bulk compositions of the films. It is noteworthy that the Ti compositions as determined by XPS are always higher (vs the light elements) in comparison to the results obtained by using bulk analytical techniques such as RBS and EMA. This may be due to preferential sputtering.[10]

In general, the bulk compositions of the films made from $Ti(NMe_2)_4$ and $Ti(NEt_2)_4$ are similar to those previously reported by Sugiyama.[4]

$Ti(NMe_2)_4$, $Ti(NEt_2)_4$, and $Ti(NMe_2)_3(t\text{-Bu})$ as Precursors. Light-Element Bonding by XPS Analysis. With regard to the nature of the incorporated light elements, all of the films gave XPS nitrogen 1s peaks at a binding energy consistent with titanium-bound nitrogen (e.g., see Figure 4). Examination of the XPS carbon 1s region for films deposited from $Ti(NMe_2)_4$ and $Ti(NEt_2)_4$

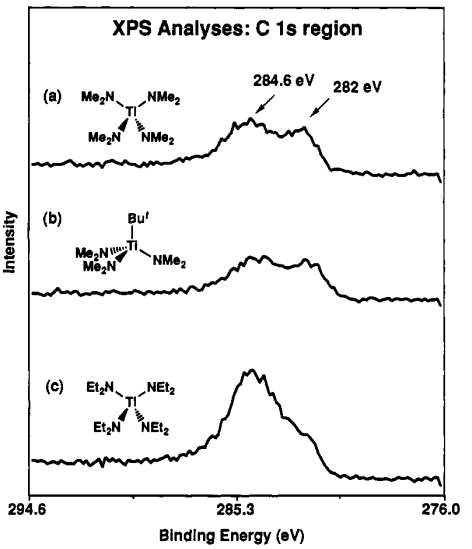

Figure 5. C 1s region of the X-ray photoelectron spectra for films deposited on silicon wafers at 400 °C with respectively **1** (a), **3** (b), and **2** (c) as precursors.

(e.g., see Figure 5a,c) revealed peaks at binding energies of 282 and 284.6 eV that are characteristic of carbon attached to titanium and organic carbon, respectively.[11] By titanium-bound carbon we mean any carbon in the coordination sphere of titanium (e.g., Ti—CH_2— and Ti=CH— groups or TiC (carbide)), whereas organic carbon refers to any carbon not in the coordination sphere of titanium (e.g., carbon attached only to another carbon, nitrogen, or oxygen). It is particularly noteworthy that more organic carbon is found in the films prepared from $Ti(NEt_2)_4$ than from $Ti(NMe_2)_4$. Also noteworthy is the fact that the carbon in the films prepared from $Ti(NMe_2)_3(t\text{-Bu})$ and $Ti(NMe_2)_4$ has similar bonding, as well as being similar in quantity; that is, the amounts of organic and titanium-bound carbon are not significantly different for films made from $Ti(NMe_2)_4$ and $Ti(NMe_2)_3(t\text{-Bu})$ (cf. Figure 5a,b).

Mechanistic Speculation. We can rationalize some of our results on the basis of well-known decomposition pathways available to the precursors:

1. Because the amount of carbon contamination is nearly the same for films made from $Ti(NMe_2)_3(t\text{-Bu})$ and $Ti(NMe_2)_4$, the *t*-butyl group must leave cleanly in the decomposition process. Two reasonable mechanisms to account for this, alkyl β-hydrogen elimination and homolytic Ti-CMe_3 bond cleavage, are illustrated in eqs 3a and 3b, respectively.[12]

$$Ti(NMe_2)_3(t\text{-Bu}) \rightarrow TiH(NMe_2)_3 + Me_2C{=}CH_2 \rightarrow Ti(NMe_2)_2 + HNMe_2 \quad (3a)$$

$$Ti(NMe_2)_3(t\text{-Bu}) \rightarrow Ti(NMe_2)_3 + Me_3C^{\bullet} \quad (3b)$$

2. Because the chemical compositions of the films made from **1** and **3** do not vary appreciably, it appears that a common intermediate is involved in the decomposition

(10) An excellent discussion concerning the problems involved with sputtering can be found in: Feldman, L. C.; Mayer, J. W. *Fundamentals of Surface and Thin Film Analysis*; North Holland: New York, 1986.

(11) Ramqvist, L.; Hamrin, K.; Johansson, G.; Fahlman, A.; Nordling, C. *J. Phys. Chem. Solids* **1969**, *30*, 1835; Wagner, C. D.; Riggs, W. M.; Davis, L. E.; Moulder, G. F.; Muilenberg, G. E. *Handbook of X-Ray Photoelectron Spectroscopy*; Perkin-Elmer Corp.: Eden Prairie, MN, 1979; p 38. See also ref 5.

(12) Collman, J. P.; Hegedus, L. S.; Norton, J. R.; Finck, R. G. *Principles and Applications of Organotransition Metal Chemistry*; University Science Books: Mill Valley, CA, 1987.

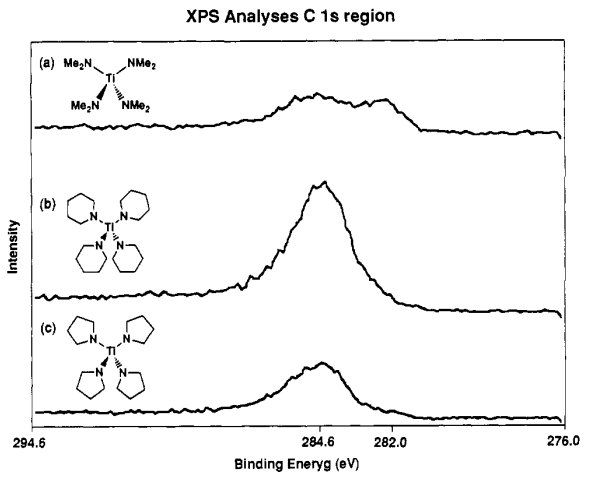

Figure 6. C 1s region of the XPS spectra for films deposited on silicon wafers at 400 °C with respectively 1 (a), 5 (b), and 4 (c) as precursors.

processes. Reasonable possibilities are $Ti(NMe_2)_2$ or $Ti(NMe_2)$.

3. The XPS data clearly show that the nitrogen in the films is in the form of nitride (TiN) and, because there is organic carbon present, perhaps imide (Ti=NR) and amide (Ti—NR_2). The titanium-bound carbon is probably present as both carbide (TiC) and organometallic carbon (Ti—CH_2— or Ti=CH—). Organometallic fragments that result from β-hydrogen activation involving the amido ligands (eq 4) may account for some of the organic and

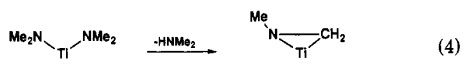

(4)

titanium-bound carbon in the films.[13] The β-hydrogen elimination process would also account for the fact that for films made from $Ti(NEt_2)_4$ vs $Ti(NMe_2)_4$, the amount of organic carbon increased but the amount of Ti-bound carbon did not.

Precursors with Cyclic Amido Ligands. If our mechanistic speculation has any validity, then two problems associated with the use of $Ti(NR_2)_4$ amido complexes as precursors in the low-temperature synthesis of TiN are readily apparent: The strong N–C bonds do not break easily, and there is facile Ti–C bond formation via β-hydrogen activation.[13]

With the latter problem in mind, new precursors were designed and synthesized (**4** and **5**). In these compounds β-hydrogen activation is hindered because the β carbons are tied back in a ring. Films were successfully synthesized by using **4** and **5** as precursors. Data obtained from XPS and RBS analyses revealed a significant increase in carbon contamination in the films. XPS analysis showed that the coatings contain titanium-bound nitrogen and organic carbon, but little or no titanium-bound carbon (cf., Figures 5 and 6). This suggests that the heterocyclic groups are leaving as radicals,[14] and the N–C bonds in the heterocyclic ligands do not cleave, thereby leaving intact $TiNC_xH_{2x}$ fragments in the films. These results show that titanium cyclic amide precursors reduce the titanium-bound carbon content.

Although the use of cyclic amido ligands in the precursors apparently blocked the β-hydrogen activation pathway, organic carbon was still incorporated because of the unreactive N–C bonds. Taking this problem into consideration, one might conjecture that amido ligands with nitrogen substituents that are good leaving groups may be well-behaved precursors. For instance, diisopropylamido, di-*tert*-butylamido, and diallylamido ligands are possibilities. In tetrakis(di-*tert*-butylamido)titanium and tetrakis(diisopropylamido)titanium the alkyl substituent would presumably leave as stabilized tertiary and secondary radicals, respectively. Unfortunately, we were unable to synthesize tetrakis(diisopropylamido)titanium to test this hypothesis, probably because of excessive steric crowding around the titanium center. For this reason we did not attempt to prepare the di-*tert*-butylamido derivative. In tetrakis(diallylamido)titanium the assumption was that the allyl group would leave as a resonance-stabilized radical. We synthesized $Ti(NCH_2CHCH_2)_4$, a dark red oily liquid, but it decomposed upon heating (via polymerization?). The thermal sensitivity and its low volatility precluded its use as a CVD precursor.

Imido Titanium(IV) Precursor. Taking into account the requirement for good leaving groups on the nitrogen ligand and considering the fact that imido-to-metal multiple bonds are stronger than amido-to-metal multiple bonds, we used $[Ti(N\text{-}t\text{-}Bu)(NMe_2)_2]_2$ (**6**) as a film precursor. We expected that the dimethylamido ligands in this complex would leave in preference to the imido ligands and that the *t*-Bu nitrogen substituent would leave as the stabilized tertiary radical.

Films were successfully prepared from **6** and, interestingly, the chemical compositions of films are not significantly different from the compositions of films prepared from **1** and **3** (Table III). Also, integration of the XPS C 1s region showed approximately the same amounts of organic and titanium-bound carbon as for **1** and **3**. These data suggest that the mechanism of decomposition for the three precursors involves the same common intermediate, perhaps $Ti(NMe_2)_2$ or $Ti(NMe_2)$, as mentioned earlier.

Conclusion

We have prepared films on glass, silicon wafer, vitreous carbon, and boron substrates by APCVD using amido and imido titanium(IV) precursors. The films, which range in thickness from 1000 to 5000 Å, are 5–10 times less conductive than pure CVD TiN and show good adhesion. Electron microprobe, RBS, and XPS analyses provide complementary data for the complete characterization of the films. In particular, we have shown that with the use of boron substrates, RBS is an excellent analytical tool for light element analysis.

The films all have Ti/N ratios close to 1 but contain significant oxygen and carbon contamination. Precursors with dialkylamido ligands give films containing both organic and titanium-bound carbon, whereas the carbon in the films made from precursors with cyclic amido ligands is primarily organic carbon. The difference can be rationalized on the basis of two distinct precursor decomposition pathways: amido ligand β-hydrogen activation in the precursors with dialkylamido ligands and homolytic Ti–N bond cleavage in the precursors with cyclic amido ligands. The presence of a *tert*-butyl ligand in one of the precursors did not increase the amount of carbon in the films in comparison to those made from precursors without the alkyl ligand. This indicates that the *tert*-butyl ligand

(13) (a) Takahashi, Y.; Onoyama, N.; Ishikawa, Y.; Motojima, S.; Sugiyama, K. *Chem. Lett.* **1978**, 525. (b) Bürger, H.; Neese, H.-J. *J. Organomet. Chem.* **1970**, *21*, 381. (c) Girolami, G. S.; Jensen, J. A.; Gozum, J. E.; Pollina, D. M. *Mater. Res. Soc. Proc.* **1988**, *121*, 429.
(14) Bradley, D. C.; Thomas, I. M. *Can. J. Chem.* **1962**, *40*, 1355.
(15) For a clean route to TiN at low temperatures, see: Fix, R. M.; Gordon, R. G.; Hoffman, D. M. *Mater. Res. Soc., Symp. Proc.*, in press.

is removed cleanly in the precursor decomposition, probably via alkyl β-hydrogen activation or homolytic Ti-C bond cleavage.[15]

Acknowledgment. We are grateful to the National Science Foundation (DMR-8802306) for support of this work. R.M.F. thanks ICI Americas for a summer fellowship. We thank David A Lange for the electron microprobe measurements. XPS and RBS analyses were carried out at the facilities of the Harvard Materials Research Laboratory, an NSF-funded facility (DMR-86-14003).

Registry No. 1, 3275-24-9; 2, 4419-47-0; 6, 70024-36-1; Ti(NMe$_2$)$_3$(*t*-Bu), 126083-69-0; TiN, 25583-20-4.

Preparation and Pyrolysis of a Polymeric Precursor for the Formation of TiN-TiC Solid Solutions

C. Rüssel

Institut für Werkstoffwissenschaften III (Glas und Keramik), Universität Erlangen—Nürnberg, Erlangen, FRG

Received June 27, 1989

Metallic titanium was anodically dissolved in an organic electrolyte containing *n*-propylamine. A highly viscous solution was formed. Heating of the fluid led to the formation of an amorphous solid. Calcination of this precursor in an atmosphere of anhydrous ammonia resulted in the formation of a gold-colored titanium nitride-titanium carbide solid solution with a comparably low carbon content, about 5%. When the calcination was carried out in nitrogen, Ti(C,N) solid solutions containing large amounts of carbon were obtained. Calcining at comparably low temperatures led to products with an extremely small crystallite size.

Introduction

Titanium nitride has some remarkable properties such as extreme hardness and excellent electrical conductivity.[1,2] At the moment, TiN is predominantly used as a cutting tool material. TiN coatings on metals, or even transition-metal carbides such as WC, are quite suitable as antiabrasive layers. For electronic applications, thin TiN layers are used as conductors. Thin TiN layers on various ceramic materials, including glass, might be used for optical and optoelectronical devices.

TiN is cubic (a = 0.4239 nm)[3] and forms solid solutions with TiC, which also has a cubic lattice with a slightly larger lattice constant (a = 0.4330 nm). Over a wide range, TiO is soluble in TiN, TiC, or TiN/TiC solid solutions.[4]

A complete absence of carbon contamination is generally not required for all applications of TiN. For some special mechanical applications, TiN/TiC solid solutions are preferable.[5]

At the moment, TiN is produced either by direct nitridation of metallic titanium or by the reaction of titanium halides of hydride with anhydrous ammonia or nitrogen/hydrogen mixtures.[6] The temperatures required for the formation of TiN are usually higher than 1000 °C. Presently, TiN coatings are formed by sputter or chemical vapor deposition (CVD) techniques. It should be noted that a method for the preparation of TiN by thermal decomposition of gaseous titanium tetrakis(dialkylamides),[7] which allows much lower formation temperatures, has already been described in literature.

The thermal decomposition of polymeric titanium precursors to TiN has also been described.[8] However, the formation temperatures were at least 1100 °C, and additional phases containing oxygen, such as Ti_3O_5, occur up to temperatures of 1400 °C. It may be assumed that this effect is due to the use of a precursor, containing large amounts of oxygen. This paper introduces a method for the formation of TiN and TiN/TiC solid solutions by pyrolysis of a polymeric oxygen-free precursor at comparably low temperatures. A quite similar method has already been developed for the formation of aluminum nitride.[9,10]

Experimental Section

Anodic Dissolution of Metallic Titanium. Metallic titanium was anodically dissolved in a purely organic electrolyte. It consists of a primary organic amine (e.g., *n*-propylamine), acetonitrile to increase the polarity, and tetrabutylammonium bromide as a supporting electrolyte to achieve sufficient electrical conductivity, necessary to reduce ohmic drops. Figure 1 shows the apparatus used for the electrolysis. A double-walled glass vessel contained the electrolyte and the electrodes. Sheets of metallic titanium (thickness 1 mm) were used for both the cathodes and anodes. The distance between two electrodes was also 1 mm. Alternate sheets were connected, and the polarity of the dc power supply was reversed every 15 min to achieve a uniform dissolution of all electrodes. A condenser, fixed to the top of the vessel, recovered solvent and excess amine, which were vaporized or carried along with the gas stream. The electrolysis was carried out without stirring in a volume of about 150 mL of electrolyte and a total electrode area of about 60 cm^2. The current density was 67 mA/cm^2 and the applied dc voltage in the range 5–6 V. For about 3 h, the current remained nearly constant and then decreased, due to an increasing viscosity of the solution. Then the electrolysis

(1) Grewe, H.; Koloska, J. Hartstoffe. In *Handbuch der Keramik*; Verlag Schmidt: Freiburg, 1983; Vol. II K3, pp 1ff.
(2) Toth, L. *Transition Metal Carbides and Nitrides*; Academic Press: New York, 1971; pp 176ff.
(3) Christensen, A. *J. Cryst. Growth* **1976**, *33*, 99.
(4) Duwez, P.; Odell, F. *J. Electrochem. Soc.* **1950**, *97*, 299.
(5) Schedler, W. *Hartmetall für den Praktiker*; VDI-Verlag: Düsseldorf, 1988; p 224ff.
(6) Powell, C. F.; Oxley, J. H.; Blocker, J. M. *Vapor Deposition*; Wiley: New York, 1966.
(7) Sugiyama, K.; Pac, S.; Takahashi, Y.; Motojima, S. *J. Electrochem. Soc.* **1975**, *122*, 1545.
(8) Kuroda, K.; Tanaka, Y.; Sugahara, Y.; Kato, C. Better Ceramics Through Chemistry III. *Mater. Res. Soc. Symp. Proc.* **1988**, *121*, 575.
(9) Seibold, M.; Rüssel, C. Better Ceramics Through Chemistry III. *Mater. Res. Soc. Symp. Proc.* **1988**; *121*, 477.
(10) Seibold, M.; Rüssel, C. *J. Am. Ceram. Soc.* **1989**, *72*, 1503.

0897-4756/90/2802-0241$02.50/0